

# Frequency-Domain Subspace Identification of Linear Time-Periodic (LTP) Systems

İsmail Uyanık, Uluç Saranlı, M. Mert Ankaralı, Noah J. Cowan and Ömer Morgül, *Member, IEEE*,

**Abstract**—This paper proposes a new methodology for subspace-based state-space identification for linear time-periodic (LTP) systems. Since LTP systems can be lifted to equivalent linear time-invariant (LTI) systems, we first lift input–output data from the unknown LTP system as if it was collected from an equivalent LTI system. Then, we use frequency-domain subspace identification methods to find an LTI system estimate. Subsequently, we propose a novel method to obtain a time-periodic realization for the estimated lifted LTI system by exploiting the specific parametric structure of Fourier series coefficients of the frequency-domain lifting method. Our method can be used to both obtain state-space estimates for unknown LTP systems as well as to obtain Floquet transforms for known LTP systems.

**Index Terms**—System identification, subspace methods, time-varying systems, linear time-periodic systems.

## I. INTRODUCTION

In this paper, we introduce a frequency-domain subspace-based state-space identification method for linear time-periodic (LTP) systems. Many problems in engineering and biology, such as wind turbines [1], rotor bearing systems [2], aircraft models [3], locomotion [4, 5], and power distribution networks [6] require the consideration of time-periodic dynamics. As such, the analysis, identification, and control of LTP systems have received considerable attention [7–9].

Pioneering work by Wereley [7] introduced a frequency-domain analysis method for LTP systems. In this work, time-periodic system matrices in the LTP state-space formulation were expanded into their Fourier series coefficients. The principle of harmonic balance was used to obtain the concept of harmonic transfer functions (HTFs). Wereley’s initial formulation for continuous-time LTP systems as infinite-dimensional operators was subsequently adapted to discrete time, which conveniently leads to finite-dimensional HTFs [10].

Most existing literature on LTP system identification [2, 11], including our own prior work on identification of legged locomotion [12–14], focuses on using input–output HTF representations rather than state space. In addition, there are also contributions to state-space-based system identification for LTP systems [15, 16], analogous to subspace identification

İsmail Uyanık is with the Laboratory of Computational Sensing and Robotics, Johns Hopkins Univ., Baltimore, MD, 21218 USA. E-mail: uyanik@jhu.edu

Uluç Saranlı is with the Dept. of Computer Eng., Middle East Technical Univ., 06800 Ankara, Turkey. E-mail: saranli@ceng.metu.edu.tr

M. Mert Ankaralı is with the Dept. of Electrical and Electronics Eng., Middle East Technical Univ., 06800 Ankara, Turkey. E-mail: mertan@metu.edu.tr

Noah J. Cowan is with the Dept. of Mechanical Eng., Johns Hopkins Univ., Baltimore, MD, 21218 USA. E-mail: ncowan@jhu.edu

Ömer Morgül is with the Dept. of Electrical and Electronics Eng., Bilkent Univ., 06800 Ankara, Turkey. E-mail: morgul@ee.bilkent.edu.tr

techniques commonly used for linear time-invariant (LTI) systems [17]. For instance, Verhaegen et al. developed a subspace identification method for estimating successive state-transition matrices from time-domain data for linear time-varying (including a special derivation for LTP) systems [15].

Critically, LTI subspace identification methods readily support both time-domain [17] and frequency-domain [18] data, whereas most subspace methods for LTP systems have focused on time-domain data [15, 16], and those state-space methods that do rely on frequency-domain data [19, 20] require that scheduling functions to be known *a priori*. To the best of our knowledge, there are no general methods for frequency-domain subspace identification of LTP systems.

Here, we present a general subspace identification methodology for estimating state-space models from frequency-domain data for LTP systems. Our proposed methodology is based on the fact that LTP systems can be represented with equivalent LTI systems via lifting [10]. Based on this observation, we first lift the input–output data of the unknown LTP system as if it was collected from an equivalent LTI system, following previous methods [10]. We then estimate a discrete-time LTI state-space equivalent for the original LTP system by using an existing LTI frequency-domain subspace identification method [18]. A key property of the frequency-domain lifting method we utilize in this paper is the specific parametric structure of Fourier series coefficients associated with the original LTP system [10]. However, this structure is not, in general, preserved during the subspace identification process due to an inevitably unknown similarity transformation. In order to solve this issue, we identify a similarity transformation for the lifted LTI system that recovers the Fourier structure although not the specific coefficients, because there is a subset of similarity transformations that preserve the Fourier structure but not its parameters. Our identification–realization algorithm also allows realizing Floquet-transformed state-space models for LTP systems with arbitrary time-periodic system matrices (see Remark 3), whose analytic derivations are often very challenging and may even be impossible [21].

This paper is outlined as follows. We introduce the problem formulation in Section II. Then in Section III, we show the existence of an equivalent discrete-time LTI system for a given LTP system via lifting, and estimate its system matrices from frequency-domain data. In Section IV, we present a novel LTP realization algorithm for the estimated lifted LTI system. We provide an illustrative numerical example and comparative analysis in Section V. Finally, we give our concluding remarks in Section VI.

## II. PROBLEM FORMULATION

In this paper, we consider single-input/single-output (SISO), stable, linear time-periodic (LTP) systems represented by

$$\begin{aligned}\dot{\bar{x}}(t) &= \bar{A}(t)\bar{x}(t) + \bar{B}(t)u(t), \\ y(t) &= \bar{C}(t)\bar{x}(t) + \bar{D}(t)u(t),\end{aligned}\quad (1)$$

where  $u(t) \in \mathbb{R}$ ,  $y(t) \in \mathbb{R}$  and  $\bar{x}(t) \in \mathbb{R}^{n_p}$  represent input, output and state vectors, respectively. The system matrices are periodic with a fixed common period  $T > 0$  (see Section III-B for the computation of  $T$ ), with  $\bar{A}(t) = \bar{A}(t+nT)$ ,  $\bar{B}(t) = \bar{B}(t+nT)$ ,  $\bar{C}(t) = \bar{C}(t+nT)$  and  $\bar{D}(t) = \bar{D}(t+nT)$ ,  $\forall n \in \mathbb{Z}$ .

We formulate the identification problem as follows:

### Given

- a single pair of input–output signals,  $u(t)$  and  $y(t)$ , in the form of a sum-of-cosines signal containing different frequency components that provide LTP frequency response

### Estimate

- the four LTP system matrices that will be equivalent to (1) up to a similarity transform.

The remaining sections detail our solution methodology (see Appendix A for the procedure). Obviously, LTI subspace identification methods would result in oversimplified LTI systems due to ignorance of harmonic responses. On the other hand, one can use linear time-varying (LTV) subspace identification methods in the time domain to solve a discrete-time version of this problem [15, 16]. Our solution method is unique in that it solves the problem in the frequency domain and results in intuitive state-space estimates in Floquet-transformed form.

## III. EXISTENCE AND ESTIMATION OF A DISCRETE-TIME LIFTED LTI SYSTEM REPRESENTATION

This section first introduces a system of transformations that needs to be used to prove the existence of a real-valued discrete-time LTI representation of (1). We then show how we estimate such an LTI system using input–output data of the original LTP system. Naturally, the original state-space form of (1) will not be available. Therefore, the transformations described in this section are not directly applied on the state-space form of (1); rather the transformations map the input–output data into a form that makes it as if they were collected from the transformed (LTI) system.

Based on Floquet theory, there exists a transformation that converts (1) into the form

$$\begin{aligned}\dot{\mathbf{x}}(t) &= \mathbf{A}\mathbf{x}(t) + \mathbf{B}(t)u(t), \\ y(t) &= \mathbf{C}(t)\mathbf{x}(t) + \mathbf{D}(t)u(t),\end{aligned}\quad (2)$$

where  $\mathbf{A}$ ,  $\mathbf{B}(t)$ ,  $\mathbf{C}(t)$  and  $\mathbf{D}(t)$  can be obtained as real-valued (by doubling the system period if necessary) as long as the system matrices in (1) are real-valued [21]. Note that deriving a Floquet transform is challenging even when the state-space is known. On the other hand, the Floquet transform is a similarity transformation and does not affect input–output data. Hence, we assume without loss of generality that the LTP system to be identified has the state-space form in (2). Note that Floquet-transformed forms are easier to work with since they have a time-invariant state matrix. Thus, we seek to find an LTP state-space estimate for (1) in a Floquet form such as (2).

### A. Discretization via Bilinear (Tustin) Transform

In principle, we could directly lift (2) to a continuous-time LTI equivalent and utilize continuous-time LTI subspace identification methods. However, the Hankel (data) matrices used for continuous-time LTI systems may become ill-conditioned with increasing system dimension [22]. Therefore, we find it more convenient to work with discrete-time LTI systems. To this end, we transform (2) to an approximate discrete-time LTI system. This has two benefits. First, lifting discrete-time LTP systems yields finite-dimensional LTI representations, unlike infinite-dimensional ones in continuous-time models. Second, and more importantly, it generalizes the applicability of our solutions to both continuous-time and discrete-time LTP systems. To accomplish this, we utilize the time-varying bilinear (Tustin) transformation to obtain a discrete-time LTP state-space representation of (2). Note that (2) is a special case of LTV systems with time-periodic system matrices (and time-invariant state matrix). Therefore, our special case reduces the transformations in [23] to

$$\begin{aligned}\mathbf{x}_d[k+1] &= \mathbf{A}_d\mathbf{x}_d[k] + \mathbf{B}_d[k]\mathbf{u}_d[k], \\ \mathbf{y}_d[k] &= \mathbf{C}_d[k]\mathbf{x}_d[k] + \mathbf{D}_d[k]\mathbf{u}_d[k],\end{aligned}\quad (3)$$

where  $\mathbf{x}_d[k]$  represents discrete-time states and

$$\begin{aligned}\mathbf{A}_d &= ((2/T_s)I + \mathbf{A})((2/T_s)I - \mathbf{A})^{-1}, \\ \mathbf{B}_d[k] &= (2/\sqrt{T_s})((2/T_s)I - \mathbf{A})^{-1}\mathbf{B}(kT_s), \\ \mathbf{C}_d[k] &= (2/\sqrt{T_s})\mathbf{C}(kT_s)((2/T_s)I - \mathbf{A})^{-1}, \\ \mathbf{D}_d[k] &= \mathbf{D}(kT_s) + \mathbf{C}(kT_s)((2/T_s)I - \mathbf{A})^{-1}\mathbf{B}(kT_s).\end{aligned}\quad (4)$$

Here,  $T_s$  is the sampling period yielding sampled input–output data as  $\mathbf{u}_d[k] := u(kT_s)$  and  $\mathbf{y}_d[k] := y(kT_s)$ . Derivations for (3) can be found in [24]. Note that (3) is an LTP system, where  $\mathbf{B}_d[k] = \mathbf{B}_d[k+nN]$ ,  $\forall n \in \mathbb{Z}$  (also valid for  $\mathbf{C}_d[k]$  and  $\mathbf{D}_d[k]$ ) and  $N$  is the discrete-time system period defined as  $N := T/T_s$ . For the sake of simplicity,  $N$  is assumed to be even. The sampling period,  $T_s$  determines  $N$  and hence the dimension of the lifted LTI equivalent. Using higher sampling frequency allows capturing high frequency dynamics but also increases the complexity by increasing the lifted LTI system dimension. In addition, bilinear (Tustin) transformation causes frequency warping (distortions) at higher frequencies. To avoid this problem, we utilize the experimental design procedure of [25] by first pre-warping the input frequencies that will be used while designing the sum-of-cosines input.

### B. Lifting to a Time-Invariant Reformulation

One of the key properties of LTP systems is that a complex exponential input with frequency  $\omega$  produces output not only at the input frequency (which is the case for LTI systems), but also at different harmonics  $\omega \pm k\omega_p$ ,  $k \in \mathbb{Z}$  separated by the system frequency,  $\omega_p = 2\pi/T$ , with possibly different magnitudes and phases in steady-state (this also allows estimating  $T$  from input–output data). In this context, the concept of Harmonic Transfer Functions (HTFs) was developed to represent each harmonic response of the LTP system with a distinct transfer function  $G_k(\omega + k\omega_p)$  for  $k \in \mathbb{Z}$  [7]. This approach represents an LTP system as the superposition of multiple modulated LTI systems. As such, HTFs can be

used as a lifting technique to transform an LTP system to an LTI equivalent [10]. This motivates our use of HTFs as the frequency-domain lifting method to obtain an LTI equivalent state-space model for (3). Among possible alternatives (see [10] for a survey), we use frequency lifting in state space due to the convenient structure of Fourier series coefficients for periodic system matrices in lifted (semi)-Toeplitz matrices.

The lifting method starts by analyzing the input–output spectra of the LTP systems by referring the concept of exponentially modulated periodic (EMP) signals. An input signal,  $\mathbf{u}_d[k]$  is a discrete-time EMP signal if there is a nonzero complex number  $z$  such that

$$\mathbf{u}_d[k + pN] = \mathbf{u}_d[k]z^{pN} \quad (5)$$

over one period for  $p \in \mathbb{Z}$  and can be written as

$$\mathbf{u}_d[k] := z^k \sum_{n=-N/2}^{N/2-1} U_n e^{j2\pi \frac{nk}{N}}, \quad (6)$$

where  $U_n$  are called modulated Fourier series coefficients for EMP signals and are defined as

$$U_n := \frac{1}{N} \sum_{k=0}^{N-1} (\mathbf{u}_d[k] z^{-k}) e^{-j2\pi \frac{nk}{N}}. \quad (7)$$

It has been shown that when an LTP system is given an EMP input, state and output signals are also EMP in steady-state [7]. Therefore, similar to (6), we obtain the state vector

$$\mathbf{x}_d[k] = z^k \sum_{n \in \mathbf{I}_N} X_n e^{j2\pi \frac{nk}{N}}, \quad (8)$$

and a similar expression for  $\mathbf{y}_d[k]$  where  $\mathbf{I}_N$  defines the interval  $\mathbf{I}_N = [-N/2, N/2 - 1]$ . In addition, discrete-time Fourier synthesis equation for  $\mathbf{B}_d[k]$  is computed as

$$\mathbf{B}_d[k] = \sum_{n \in \mathbf{I}_N} B_n e^{j2\pi \frac{nk}{N}}. \quad (9)$$

Similar expressions are also valid for  $\mathbf{C}_d[k]$  and  $\mathbf{D}_d[k]$ . Substituting Fourier synthesis equations into (3) yields

$$0 = z^k \sum_{n \in \mathbf{I}_N} \left( z X_n e^{j2\pi \frac{nk}{N}} - \mathbf{A}_d X_n - \sum_{m \in \mathbf{I}_N} B_{n-m} U_m \right) e^{j2\pi \frac{nk}{N}}. \quad (10)$$

The exponentials  $\{e^{j2\pi \frac{nk}{N}} \mid n \in \mathbf{I}_N\}$  constitute an orthonormal basis. Thus, by the principle of harmonic balance, each term enclosed by the brackets must be zero to ensure that the overall sum is zero. Therefore, for all  $n \in \mathbf{I}_N$ , we have

$$z e^{j2\pi \frac{nk}{N}} X_n = \mathbf{A}_d X_n + \sum_{m \in \mathbf{I}_N} B_{n-m} U_m. \quad (11)$$

Note that the above equation is valid since Fourier coefficients,  $B_m$ , are also periodic with  $N$ . For the output, we also have

$$Y_n = \sum_{m \in \mathbf{I}_N} C_{n-m} X_m + \sum_{m \in \mathbf{I}_N} D_{n-m} U_m \quad (12)$$

for all  $n \in \mathbf{I}_N$ . Similar to continuous-time systems, (11) and (12) can be represented with (semi)-Toeplitz matrices to obtain an LTI state-space model. To this end, we first define the  $N$ -block state ( $\mathcal{X}_d$ ), input ( $\mathcal{U}_d$ ) and output ( $\mathcal{Y}_d$ ) vectors, whose  $i^{\text{th}}$  block for  $i = 1, 2, \dots, N$  are given as

$$\mathcal{X}_d(i) = X_{i-1-\frac{N}{2}}, \quad \mathcal{U}_d(i) = U_{i-1-\frac{N}{2}}, \quad \mathcal{Y}_d(i) = Y_{i-1-\frac{N}{2}}. \quad (13)$$

In addition, time-invariant reformulation of the unlifted  $N$ -periodic output matrix can be obtained as

$$\mathbf{C}_d := \begin{bmatrix} C_0 & C_{-1} & \dots & C_{-\frac{N}{2}} & C_{\frac{N}{2}-1} & C_{\frac{N}{2}-2} & \dots & C_1 \\ C_1 & C_0 & \dots & C_{-\frac{N}{2}+1} & C_{-\frac{N}{2}} & C_{\frac{N}{2}-1} & \dots & C_2 \\ \vdots & \vdots & & \vdots & \vdots & \vdots & & \vdots \\ C_{-1} & C_{-2} & \dots & C_{\frac{N}{2}-1} & C_{\frac{N}{2}-2} & C_{\frac{N}{2}-3} & \dots & C_0 \end{bmatrix}. \quad (14)$$

Similarly, (semi)-Toeplitz forms for  $\mathcal{B}_d$  and  $\mathcal{D}_d$  matrices can be obtained in terms of their Fourier series coefficients,  $\{B_n \mid n \in \mathbf{I}_N\}$  and  $\{D_n \mid n \in \mathbf{I}_N\}$ , respectively. Note that, since  $\mathbf{A}_d$  is time-invariant, its Toeplitz form,  $\mathcal{A}_d$  includes only  $\mathbf{A}_d$  in its diagonals as

$$\mathcal{A}_d := \text{blkdiag}\{\mathbf{A}_d\} \mid \mathcal{A}_d \in \mathbb{R}^{Nn_p \times Nn_p}, \quad (15)$$

where *blkdiag* represents a block-diagonal matrix and  $\mathbf{A}_d$  is repeated block-wise on diagonals. Lastly, we define a modulation matrix,  $\mathcal{N}_d$  to capture the exponential terms in (11) as

$$\mathcal{N}_d := \text{blkdiag}\{e^{j2\pi \frac{nk}{N}} I_{n_p} \mid \forall n \in \mathbf{I}_N\}. \quad (16)$$

We also define

$$\mathcal{A}_{dN} := \mathcal{N}_d^{-1} \mathcal{A}_d, \quad \mathcal{B}_{dN} := \mathcal{N}_d^{-1} \mathcal{B}_d. \quad (17)$$

Now, (11) and (12) can be represented as

$$\begin{aligned} z \mathcal{X}_d &= \mathcal{A}_{dN} \mathcal{X}_d + \mathcal{B}_{dN} \mathcal{U}_d, \\ \mathcal{Y}_d &= \mathcal{C}_d \mathcal{X}_d + \mathcal{D}_d \mathcal{U}_d. \end{aligned} \quad (18)$$

This is called the harmonic state-space (HSS) model and it represents a lifted LTI equivalent of (1) for a general class of input–output signals. Next sections explain how we transform this HSS model to a more intuitional single-input multi-output (SIMO) LTI equivalent by limiting the space of EMP inputs.

### C. A Single-Input Multi-Output (SIMO) LTI Equivalent

The input to the original LTP system (1) is a sum-of-cosines signal in the form  $u(t) = \sum_{m=1}^M 2K \cos(\omega_m t)$ . As stated earlier, each cosine input at  $\omega_m$  produces an output spectra at  $\pm\omega_m \pm k\omega_p$  for  $k \in \mathbb{Z}$ , since cosine triggers both  $\pm\omega_m$ . Hence the input frequencies should be carefully selected to avoid any coincidence of harmonic responses (see [26] for illustrative explanations). Once this is satisfied, we can separate the input–output response of each individual cosine signal in frequency domain. At this point, we write each single cosine input as

$$u_c(t) = 2K \cos(\omega_m t) = \underbrace{K e^{j\omega_m t}}_{u_c^+(t)} + \underbrace{K e^{-j\omega_m t}}_{u_c^-(t)}. \quad (19)$$

Let the output of (1) to inputs  $u_c^+(t)$ ,  $u_c^-(t)$  and  $u_c(t)$  be  $y_c^+(t)$ ,  $y_c^-(t)$  and  $y_c(t)$ , respectively where  $y_c(t) = y_c^+(t) + y_c^-(t)$ . Ensuring that  $\omega_m \neq 0.5k\omega_p$  for  $k \in \mathbb{Z}$ , one can also guarantee that there will be no coincidence in harmonic responses of the single-cosine input [26]. Thus, we can simulate (1) with  $u_c(t)$  and only use  $y_c^+(t)$  as the output assuming that our input was  $u_c^+(t)$ . We choose distinct exponential modulation,  $z = e^{j\omega_m}$  in (5) for each individual input signal. Hence, the modulated Fourier series coefficient vector in (18) becomes  $\mathcal{U}_d = [0 \dots 0 K 0 \dots 0]^T$  with  $K$  on row  $(N/2+1)$  for each input. More importantly, with its current form,  $\mathcal{U}_d$  selects only column  $(N/2+1)$  in (14) for  $\mathcal{B}_d$  and  $\mathcal{D}_d$ , yielding

$$\begin{aligned} z \mathcal{X}_d &= \mathcal{A}_{dN} \mathcal{X}_d + \bar{\mathcal{B}}_{dN} \bar{\mathcal{U}}_d, \\ \mathcal{Y}_d &= \mathcal{C}_d \mathcal{X}_d + \bar{\mathcal{D}}_d \bar{\mathcal{U}}_d, \end{aligned} \quad (20)$$

where  $\bar{U}_d = K$ ,  $z = e^{j\omega_m}$ , and

$$\begin{aligned} \bar{B}_{dN} &:= \mathcal{N}_d^{-1} [B_{-N/2} \ \dots \ B_0 \ \dots \ B_{N/2-1}]^T, \\ \bar{D}_d &:= [D_{-N/2} \ \dots \ D_0 \ \dots \ D_{N/2-1}]^T. \end{aligned} \quad (21)$$

#### D. Transforming to a Real-Valued State-Space Model

One problem with LTI subspace identification methods is that they rely on real-valued input–output data in the time domain to estimate real-valued system matrices [27–31]. Hence, we need to transform (20) to a system that, if it were converted to time-domain, would produce real-valued states and outputs given real-valued inputs. Note that this system would not correspond to our original time-domain system. Rather, the time-domain equivalent of (20) is a fictitious system, useful only for the purpose of analysis. This SIMO LTI system has  $N$  states and outputs:

$$\begin{aligned} \mathcal{X}_d[k] &:= [\bar{\mathcal{X}}_{-N/2}[k] \ \dots \ \bar{\mathcal{X}}_0[k] \ \dots \ \bar{\mathcal{X}}_{N/2-1}[k]]^T, \\ \mathcal{Y}_d[k] &:= [\bar{\mathcal{Y}}_{-N/2}[k] \ \dots \ \bar{\mathcal{Y}}_0[k] \ \dots \ \bar{\mathcal{Y}}_{N/2-1}[k]]^T. \end{aligned} \quad (22)$$

Considering (20) as an LTI system in the  $z$ -domain and by utilizing the block-diagonal structure of  $\mathcal{A}_{dN}$  (noting that  $\mathbf{A}_d$  is stable), one can simply solve for each state equation in steady state as

$$\bar{\mathcal{X}}_m[k] = \sum_{i=0}^{k-1} (e^{-j2\pi \frac{m}{N}} I_{n_p} \mathbf{A}_d)^{k-i-1} (e^{-j2\pi \frac{m}{N}} I_{n_p} B_m) u[i] \quad (23)$$

where  $u[k] = 2K \cos(\omega_m k T_s)$ . This follows since  $\bar{U}_d = K$  in the  $z$ -domain corresponds to a single cosine input signal for the time-domain signal. (We write the input as in (19) and ignore the negative frequency component for the sake of our analysis). Also note that  $B_m = B_{-m}^*$ , since  $\mathbf{B}_d[k]$  is real-valued by definition. Hence, we can state that  $\bar{\mathcal{X}}_m[k] = \bar{\mathcal{X}}_{-m}^*[k]$  except for  $\bar{\mathcal{X}}_{-N/2}[k]$  and  $\bar{\mathcal{X}}_0[k]$ , which are both real-valued as seen in (23). A similar analysis can be done for  $\mathcal{Y}_d[k]$  by using (23). However, solutions for each LTI output signals,  $\bar{\mathcal{Y}}_m[k]$ , is more challenging since complex-conjugate state solutions are now multiplied with shifted versions of Fourier series coefficients as illustrated in (14). To achieve our goal, we first write the steady-state solutions for each output signal as

$$\bar{\mathcal{Y}}_m[k] = \sum_{n \in \mathbf{I}_N} C_{m-n} \bar{\mathcal{X}}_n[k]. \quad (24)$$

By using lengthy but straightforward calculations, one can show that  $\bar{\mathcal{Y}}_m[k] = \bar{\mathcal{Y}}_{-m}^*[k]$  in steady state. Having shown the complex-conjugate nature of the time-domain state and output signals, we define two complex-valued transformation matrices  $\mathcal{T}_x$  and  $\mathcal{T}_y$  as

$$\underline{\mathcal{X}}_d[k] := \mathcal{T}_x \mathcal{X}_d[k], \quad \underline{\mathcal{Y}}_d[k] := \mathcal{T}_y \mathcal{Y}_d[k], \quad (25)$$

where  $\mathcal{T}_x$  can be defined as

$$\mathcal{T}_x := 0.5 \begin{bmatrix} 2I_{n_p} & 0 & 0 & 0 \\ 0 & I_{(N/2-1)n_p} & 0 & J_{(N/2-1)n_p} \\ 0 & 0 & 2I_{n_p} & 0 \\ 0 & -jJ_{(N/2-1)n_p} & 0 & jI_{(N/2-1)n_p} \end{bmatrix}, \quad (26)$$

with a similar expression for  $\mathcal{T}_y$ , where  $I_{\bar{n}}$  is the usual  $\bar{n} \times \bar{n}$  identity and  $J_{\bar{n}}$  is an anti-diagonal  $\bar{n} \times \bar{n}$  matrix (i.e. 1 for

the entries where  $i = \bar{n} - j + 1$ , 0 else) with associated sizes, respectively. Eq. (25) transforms (20) to

$$\begin{aligned} z\mathcal{X} &= \mathcal{T}_x \mathcal{A}_{dN} \mathcal{T}_x^{-1} \mathcal{X} + \mathcal{T}_x \bar{B}_{dN} \bar{U}_d, \\ \mathcal{Y} &= \mathcal{T}_y \mathcal{C}_d \mathcal{T}_x^{-1} \mathcal{X} + \mathcal{T}_y \bar{D}_d \bar{U}_d. \end{aligned} \quad (27)$$

where  $\mathcal{X} := \mathcal{T}_x \mathcal{X}_d$  and  $\mathcal{Y} := \mathcal{T}_y \mathcal{Y}_d$ . Note that  $\mathcal{T}_x$  and  $\mathcal{T}_y$  also transform the system matrices to real-valued equivalents.

#### E. Estimating an LTI Equivalent via Subspace Identification

At this point, we could utilize a variety of LTI subspace identification methods [17, 18, 27, 32, 33]. Although we could not find a general benchmarking study on these algorithms, it has been shown that CVA [18] performs better than N4SID [17] and MOESP [32] in terms of prediction error and computational complexity [34]. Moreover, CVA [18] is MATLAB's (The MathWorks, Inc., Natick, MA) built-in frequency-domain subspace identification method. Hence, we use CVA for estimating the equivalent LTI system by carefully selecting the estimated system dimension (see Remark 1).

**Remark 1.** In classical LTI subspace identification, the estimated system order,  $\hat{n}$ , is chosen based on large drops in singular values of Hankel matrices [17]. However, one needs to be aware of the specific parametric structure of LTP systems while selecting  $\hat{n}$ . Let the eigenvalues of  $\mathbf{A}_d$  be  $S_d = \{\lambda_i^d\}_{i=1}^{n_p}$ . Lifting to (17) results in  $\mathcal{A}_{dN}$  with the following eigenvalues

$$S = \left\{ \left\{ \lambda_i^d e^{-j2\pi \frac{k}{N}} \right\}_{i=1}^{n_p} \mid \forall k \in \mathbf{I}_N \right\}. \quad (28)$$

Once  $\hat{n}$  is chosen based on the singular values (not the eigenvalues), the user should check the eigenvalues of the estimated state matrix for the phase structure defined in (28). This phase structure will both reveal the underlying LTP system's dimension,  $n_p$ , as well as the number of harmonics that will appear in state vector,  $N_h$ . The user might need to use expert knowledge to decide on  $\hat{n}$  to maintain the phase structure of (28). The correct choice of  $\hat{n}$  will yield eigenvalues

$$\hat{S} = \left\{ \left\{ \lambda_i^d e^{-j2\pi \frac{k}{N}} \right\}_{i=1}^{n_p} \mid \forall k \in [-N_h, N_h] \right\}. \quad (29)$$

Note that under these constraints  $\hat{n}$  would be equal to the cardinality of  $\hat{S}$ , i.e.  $\hat{n} = |\hat{S}| = (2N_h + 1)n_p$  and this will limit the dimensions of  $\hat{\mathcal{X}}$  (and associated system matrices) in (30). It is quite possible that the user could also limit the output harmonics in (13) based on LTP frequency response. This choice will be independent of  $\hat{n}$  and it will limit the dimensions of  $\hat{\mathcal{Y}}$  (and associated system matrices) in (30).  $\square$

The CVA method estimates a quadruple of real-valued LTI system matrices as  $[\hat{A}, \hat{B}, \hat{C}, \hat{D}]$ , which is equivalent to (27) up to a similarity transformation. However, we need to back-substitute the transformations in (17) to find an equivalent lifted LTI system for the unknown LTP system. To this end, we use  $\hat{A} = \hat{A}$ ,  $\hat{B} = \hat{B}$ ,  $\hat{C} = \mathcal{T}_y^{-1} \hat{C}$  and  $\hat{D} = \mathcal{T}_y^{-1} \hat{D}$  and obtain the equivalent lifted LTI system as

$$\begin{aligned} z\hat{\mathcal{X}} &= \hat{A}\hat{\mathcal{X}} + \hat{B}\hat{U}_d, \\ \hat{\mathcal{Y}} &= \hat{C}\hat{\mathcal{X}} + \hat{D}\hat{U}_d \end{aligned} \quad (30)$$

where  $\hat{A} \in \mathbb{R}^{\hat{n} \times \hat{n}}$ ,  $\hat{B} \in \mathbb{R}^{\hat{n} \times 1}$ ,  $\hat{C} \in \mathbb{C}^{N \times \hat{n}}$  and  $\hat{D} \in \mathbb{C}^{N \times 1}$ . Note that we do not substitute  $\mathcal{T}_x$  back, since it is already in the form of a similarity transformation.

At this point, our method provides a parametric system representation, which is equivalent to the lifted LTI form (27) of the original LTP system. However, the main drawback of this representation—lifted LTI—is that it is unintuitive and requires additional processes (unlifting the signals) to predict the output of the original LTP system. In Section IV, we introduce an LTP realization method that collapses the lifted LTI system to an LTP system in Floquet form.

#### IV. TIME-PERIODIC REALIZATION FOR THE ESTIMATED LIFTED LTI EQUIVALENT

The specific parametric structure of Fourier series coefficients is not generally preserved during subspace identification. Finding a computationally effective solution to this problem remains an open issue [35]. Motivated by this, we propose a time-periodic realization method for lifted LTI systems. Unlike the previous work that considers unforced LTP systems [36], we provide a framework for a general class of LTP systems with inputs. Our goal can be defined as finding a similarity transformation matrix,  $\mathcal{T}$  such that

$$\begin{bmatrix} \mathcal{T}^{-1} & 0 \\ 0 & I \end{bmatrix} \begin{bmatrix} \hat{A} & \hat{B} \\ \hat{C} & \hat{D} \end{bmatrix} \begin{bmatrix} \mathcal{T} & 0 \\ 0 & I \end{bmatrix} = \begin{bmatrix} A_S & B_S \\ C_S & D_S \end{bmatrix}, \quad (31)$$

where  $[A_S, B_S, C_S, D_S]$  represents the parametric structure of Fourier series coefficients as defined in (14), (15) and (21).

**Assumption 1.**  $\hat{A}$  has non-repeated eigenvalues and hence it is diagonalizable via a similarity transformation matrix,  $\mathcal{T}_D$ . Note that this also constrains  $\mathbf{A}_d$  in (3) to be diagonalizable.

Assumption 1 is reasonable, since even small perturbations eliminate repeated eigenvalues. We find such a  $\mathcal{T}_D$  using an eigenvalue decomposition of  $\hat{A}$  and transform the system as

$$\begin{aligned} \hat{A}_D &= \mathcal{T}_D^{-1} \hat{A} \mathcal{T}_D, & \hat{B}_D &= \mathcal{T}_D^{-1} \hat{B}, \\ \hat{C}_D &= \hat{C} \mathcal{T}_D, & \hat{D}_D &= \hat{D}. \end{aligned} \quad (32)$$

Recall that there is a freedom in performing the eigenvalue decomposition, so when doing this, we ensure that  $\mathcal{T}_D$  is selected such that eigenvalues of  $\hat{A}_D$  enjoy the same parametric phase structure and ordering as (28). Lastly, because of the SIMO structure of the lifted system, there are additional constraints (14) on the output matrix,  $\hat{C}_D$  but not on  $\hat{B}_D$  (the input matrix is a column vector). These constraints can be satisfied with a similarity transformation,  $\mathcal{T}_C$ . Note that such a transformation should maintain the parametric form of  $\hat{A}_D$ .

**Proposition 1.** Given Assumption 1, the similarity transformation matrix,  $\mathcal{T}_C \in \mathbb{C}^{\hat{n} \times \hat{n}}$ , that satisfies

$$\mathcal{T}_C^{-1} \hat{A}_D \mathcal{T}_C = \hat{A}_D \quad (33)$$

has a diagonal structure as  $\mathcal{T}_C = \text{diag}\{\gamma_1, \gamma_2, \dots, \gamma_{\hat{n}}\}$ .

Given Assumption 1, the proof is trivial. Hence, we use  $\mathcal{T}_C$  to put  $\hat{C}_D$  into the desired parametric form  $C_S$  as

$$\hat{C}_D \mathcal{T}_C = C_S, \quad (34)$$

where  $C_S$  is the  $N \times \hat{n}$  center columns of  $C_d$  in (14). Note that  $C_S$  is still in a parametric representation. However, we know that (34) projects  $\hat{C}_D$  onto  $C_S$  such that there will be multiple equality constraints due to same complex Fourier series coefficients in main and sub diagonals as shown in (14). However, these terms will not be numerically equal due to inevitable noise and hence we first find the optimal Fourier series coefficients candidates. For simplicity, we will show the computations as if each Fourier series coefficient in  $C_S$  is a complex-valued scalar term, although they are vectors ( $\mathbb{C}^{1 \times n_p}$ ). However, each variable in these vectors individually satisfies the form of  $C_S$  and is multiplied with a different element of the diagonal similarity transformation matrix. Hence, we can process them separately and combine the results. With this in mind, we choose the candidate solutions as the mean of their occurrences in  $C_S$  as

for  $-N_h - 1 \leq m \leq N_h$

$$\bar{C}_m = \sum_{i=1}^{2N_h+1} \frac{\hat{C}_D(N/2 - N_h + m + i, i) \gamma_i}{2N_h + 1}, \quad (35)$$

for  $m > N_h$

$$\bar{C}_m = \sum_{i=1}^{3N_h+1-m} \frac{\hat{C}_D(N/2 - N_h + m + i, i) \gamma_i}{3N_h + 1 - m}, \quad (36)$$

for  $m < -N_h - 1$

$$\bar{C}_m = \sum_{i=1}^{3N_h+1+m} \frac{\hat{C}_D(i, i - N_h - 1 - m) \gamma_{(i - N_h - 1 - m)}}{3N_h + 1 + m}. \quad (37)$$

Now, we can generate  $C_S$  in terms of the estimated (and transformed) output matrix,  $\hat{C}_D$  and the diagonal similarity transformation matrix,  $\mathcal{T}_C$ . We equate each variable on the left hand side of (34) to their corresponding value in  $C_S$  using the complex Fourier series coefficients defined by (35)–(37). Note that these equalities will constrain the similarity transformation matrix,  $\mathcal{T}_C$ . However, we expect to have infinitely many solutions that satisfy (34). Therefore, we formulate the set of all possible solutions and select one towards an LTP realization of the estimated system. For instance, for the fundamental harmonic, the first equality can be written by using (35) as

$$\hat{C}_D(N/2 + 1 - N_h, 1) \gamma_1 = \sum_{i=1}^{2N_h+1} \frac{\hat{C}_D(N/2 - N_h + i, i) \gamma_i}{2N_h + 1}. \quad (38)$$

Organizing terms and multiplying both sides by  $2N_h + 1$  yields

$$2N_h \hat{C}_D(N/2 + 1 - N_h, 1) \gamma_1 = \sum_{i=2}^{2N_h+1} \hat{C}_D(N/2 - N_h + i, i) \gamma_i. \quad (39)$$

We utilize a vector form for (39) as  $\nu_0^1 \Gamma = 0$ , where

$$\begin{aligned} \nu_0^1 &:= [2N_h \hat{C}_D(N/2 + 1 - N_h, 1), -\hat{C}_D(N/2 + 2 - N_h, 2), \dots], \\ \Gamma &:= [\gamma_1, \gamma_2, \dots, \gamma_{(2N_h+1)}]^T. \end{aligned} \quad (40)$$

Here,  $\nu_0^1$  represents the coefficients of the first constraint for the 0<sup>th</sup> Fourier series coefficient. Similarly,  $i^{\text{th}}$  constraint on the 0<sup>th</sup> Fourier series coefficient can be written as

$$\nu_0^i := [\dots, -\hat{C}_D(\cdot, \cdot), 2N_h \hat{C}_D(\cdot, \cdot), -\hat{C}_D(\cdot, \cdot), \dots]. \quad (41)$$

Once we derive all constraint equations for all Fourier series coefficients, we combine in matrix multiplication form as

$$\mathcal{V} \Gamma = 0, \quad (42)$$

where  $\mathcal{V}$  includes all coefficient vectors for all complex Fourier series coefficients. We expect a complex-valued similarity transformation matrix and write (42) in real-valued form as

$$\underbrace{\begin{bmatrix} Re\{\mathcal{V}\} & -Im\{\mathcal{V}\} \\ Im\{\mathcal{V}\} & Re\{\mathcal{V}\} \end{bmatrix}}_{\bar{\mathcal{V}}} \underbrace{\begin{bmatrix} Re\{\Gamma\} \\ Im\{\Gamma\} \end{bmatrix}}_{\bar{\Gamma}} = 0. \quad (43)$$

Note that  $\bar{\mathcal{V}} \in \mathbb{R}^{(2M) \times (4N_h+2)}$ , where  $M > 2N_h + 1$ .

**Proposition 2.**  $\bar{\mathcal{V}}$  is rank deficient and hence the nullspace of  $\bar{\mathcal{V}}$  (with dimension 2) defines the subspace of similarity transformation matrices that satisfy (34).  $\square$

*Proof.* We start by replacing the RHS of (38) with  $\bar{C}_m$  to show that each  $\hat{C}_D(\cdot, \cdot)$  in  $\bar{\mathcal{V}}$  can be written in terms of  $\bar{C}_m$  (see Remark 2). Hence, we can rewrite  $\nu_0^1$  as

$$\nu_0^1 := [2N_h \bar{C}_0 / \gamma_1, -\bar{C}_0 / \gamma_2, \dots, -\bar{C}_0 / \gamma_{(2N_h+1)}]. \quad (44)$$

At this point, we can expand  $\nu_0^1$  as

$$\nu_0^1 := \underbrace{[2N_h \bar{C}_0, -\bar{C}_0, \dots, -\bar{C}_0]}_{\nu_0^1} \underbrace{\begin{bmatrix} 1/\gamma_1 & & & \\ & \ddots & & \\ & & & 1/\gamma_{(2N_h+1)} \end{bmatrix}}_{\underline{\gamma}}, \quad (45)$$

where the summation of the elements of  $\nu_0^1$  is 0. We can also apply the same expansion on  $\bar{\mathcal{V}}$  as

$$\bar{\mathcal{V}} = \underbrace{\begin{bmatrix} Re\{\underline{\mathcal{V}}\} & -Im\{\underline{\mathcal{V}}\} \\ Im\{\underline{\mathcal{V}}\} & Re\{\underline{\mathcal{V}}\} \end{bmatrix}}_{\bar{\mathcal{V}}^\dagger} \underbrace{\begin{bmatrix} Re\{\underline{\gamma}\} & -Im\{\underline{\gamma}\} \\ Im\{\underline{\gamma}\} & Re\{\underline{\gamma}\} \end{bmatrix}}_{\underline{\gamma}^\dagger} \quad (46)$$

such that the summation of columns in  $\bar{\mathcal{V}}^\dagger$  would be 0 based on (45). Thus, one of the columns can always be written in terms of the others proving that  $\bar{\mathcal{V}}$  is rank deficient.

Note that rank of  $\bar{\mathcal{V}}$  equals to the rank of  $\bar{\mathcal{V}}^\dagger$ , since  $\underline{\gamma}^\dagger$  is full rank by definition. Further, the way we define  $\bar{\mathcal{V}}^\dagger$  ensures that column space of its left and right halves are orthogonal to each other. Hence, we simply add the dimensions of nullspaces of the left and right halves to obtain the overall dimension of the nullspace of  $\bar{\mathcal{V}}$ . We know that the left and right halves are rank deficient by (45). In order to find the dimension of the nullspace of left half, we consider the constraint equations,  $\nu_0^i, \forall i = \{1, 2, \dots, 2N_h+1\}$  for  $\bar{C}_0$  only, which will generate the coefficient vectors as (also valid for  $Im\{\underline{\gamma}\}$ )

$$\begin{bmatrix} 2N_h Re\{\bar{C}_0\} & -Re\{\bar{C}_0\} & \dots & -Re\{\bar{C}_0\} \\ -Re\{\bar{C}_0\} & 2N_h Re\{\bar{C}_0\} & \ddots & -Re\{\bar{C}_0\} \\ \vdots & \ddots & \ddots & \vdots \\ -Re\{\bar{C}_0\} & \dots & \dots & 2N_h Re\{\bar{C}_0\} \end{bmatrix}. \quad (47)$$

Putting (47) to row echelon form, one can simply show that  $Re\{\underline{\mathcal{V}}\}$  is only rank-1 deficient (as  $Im\{\underline{\gamma}\}$ ). Considering the same derivations for the right half, one can find that the dimension of the nullspace of  $\bar{\mathcal{V}}$  as 2.  $\square$

**Remark 2.** Note that (35), (36) and (37) defines the ‘‘optimal’’ Fourier series coefficients as the mean of their occurrences. In the proof of Proposition 2, we assume that we can write each  $\hat{C}_D(\cdot, \cdot)$  in  $\bar{\mathcal{V}}$  in terms of  $\bar{C}_m$ . However, this equivalence is only valid for the noise free case. Noise will perturb the constraint

equations and numerically  $\bar{\mathcal{V}}$  will be full rank. The reason we computed the dimension of the nullspace is that we can use this dimension to choose the number of least significant eigenvectors of  $\bar{\mathcal{V}}$  when generating solution space for  $\bar{\Gamma}$ .  $\square$

Now, we know that dimension of the nullspace for  $\bar{\mathcal{V}}$  should be 2. Therefore, we use SVD to find the eigenvectors for  $\bar{\mathcal{V}}$ . Then, we choose 2 eigenvectors,  $v_1$  and  $v_2$ , corresponding to least significant singular values as the basis vectors of nullspace of  $\bar{\mathcal{V}}$ . Hence, the solution set for  $\bar{\Gamma}$  can be written as  $\bar{\Gamma} = \alpha_1 v_1 + \alpha_2 v_2$  and any choice of  $(\alpha_1, \alpha_2)$  pair yield a valid solution for  $\bar{\Gamma}$  that will construct the similarity transformation matrix  $\mathcal{T}_C$ , which transforms (32) to

$$\begin{aligned} \hat{A}_S &= \mathcal{T}_C^{-1} \hat{A}_D \mathcal{T}_C, & \hat{B}_S &= \mathcal{T}_C^{-1} \hat{B}_D, \\ \hat{C}_S &= \hat{C}_D \mathcal{T}_C, & \hat{D}_S &= \hat{D}_D. \end{aligned} \quad (48)$$

Given (48), we identify the Fourier series coefficients for system matrices and construct LTP state-space realization as

$$\begin{aligned} \hat{\mathbf{x}}_d[k+1] &= \hat{\mathbf{A}}_d \hat{\mathbf{x}}_d[k] + \hat{\mathbf{B}}_d[k] \mathbf{u}_d[k], \\ \hat{\mathbf{y}}_d[k] &= \hat{\mathbf{C}}_d[k] \hat{\mathbf{x}}_d[k] + \hat{\mathbf{D}}_d[k] \mathbf{u}_d[k] \end{aligned} \quad (49)$$

by using the Fourier synthesis equations such as (9). Finally, inverse bilinear (Tustin) transformation on (49) yields

$$\begin{aligned} \hat{\mathbf{x}}(t) &= \hat{\mathbf{A}} \hat{\mathbf{x}}(t) + \hat{\mathbf{B}}(t) u(t), \\ \hat{\mathbf{y}}(t) &= \hat{\mathbf{C}}(t) \hat{\mathbf{x}}(t) + \hat{\mathbf{D}}(t) u(t), \end{aligned} \quad (50)$$

where

$$\begin{aligned} \hat{\mathbf{A}} &= (2/T_s)(\hat{\mathbf{A}}_d + I)^{-1}(\hat{\mathbf{A}}_d - I), \\ \hat{\mathbf{B}}(kT_s) &= (2/\sqrt{T_s})(\hat{\mathbf{A}}_d + I)^{-1} \hat{\mathbf{B}}_d[k], \\ \hat{\mathbf{C}}(kT_s) &= (2/\sqrt{T_s}) \hat{\mathbf{C}}_d[k](\hat{\mathbf{A}}_d + I)^{-1}, \\ \hat{\mathbf{D}}(kT_s) &= \hat{\mathbf{D}}_d[k] - \hat{\mathbf{C}}_d[k](\hat{\mathbf{A}}_d + I)^{-1} \hat{\mathbf{B}}_d[k], \end{aligned} \quad (51)$$

and intersample behavior is obtained via linear interpolation.

**Remark 3.** Note that one can use this methodology to obtain Floquet transforms for known LTP systems. To accomplish this, one can simply equate the system matrices in (30) to those in (27) by skipping the LTI subspace identification part.

## V. NUMERICAL EXAMPLE

In this section, we provide a numerical example to both illustrate the practicality of the proposed method as well as to present a comparative analysis with one of the time-domain LTP subspace identification methods in the literature [15].

The numerical example we consider is in the form

$$\begin{aligned} \dot{\mathbf{x}}(t) &= \bar{A}(t) \bar{\mathbf{x}}(t) + \bar{B}(t) u(t), \\ \mathbf{y}(t) &= \bar{C}(t) \bar{\mathbf{x}}(t) \end{aligned} \quad (52)$$

with the following system matrices

$$\begin{aligned} \bar{A}(t) &= \begin{bmatrix} -2\mathbf{s}^2(t) + 0.5\mathbf{s}(2t) & \mathbf{s}(t) + \mathbf{s}(2t) \\ -\mathbf{c}^2(t) + \mathbf{s}(2t) & -2\mathbf{c}^2(t) - 0.5\mathbf{s}(2t) \end{bmatrix}, \\ \bar{B}(t) &= \begin{bmatrix} -\mathbf{s}(t)(1 + \beta_b \mathbf{c}(t)) \\ \mathbf{c}(t)(1 + \beta_b \mathbf{c}(t)) \end{bmatrix}, \\ \bar{C}(t) &= [\mathbf{c}(t)(1 + \beta_c \mathbf{c}(t)) \quad \mathbf{s}(t)(1 + \beta_c \mathbf{c}(t))], \end{aligned} \quad (53)$$

where  $\mathbf{s}(t) = \sin(4\pi t)$ ,  $\mathbf{c}(t) = \cos(4\pi t)$ ,  $\mathbf{s}(2t) = \sin(8\pi t)$ ,  $\beta_b = 0.5$  and  $\beta_c = 0.3$ .

We simulate the LTP system with a sinusoidal input signal as sum of different frequency cosine inputs. In order to design

our input signal, we first choose the sampling frequency as  $f_s = 1 \text{ KHz}$ . We plan to use the summation of 400 different frequency cosine signals in the range (0.1, 250) Hz for 200 s. Instead of choosing equidistant frequency values in continuous-time, we transform our limits to discrete-time frequency equivalents using the technique presented in [25] and then choose 400 equidistant frequency values in discrete-time to avoid distortion (warping) in high frequencies. Then, we transform the discrete-time frequency values back to continuous-time. This process is called *pre-warping* [25].

Once we obtain the input–output data from the unknown system, we apply the proposed subspace identification method to estimate an LTP realization for the original system (see Appendix A). We estimate an equivalent representation for (52) in the form of (50) with the system matrices as

$$\begin{aligned} \hat{\mathbf{A}} &= \begin{bmatrix} 0 & 1 \\ -170.4848 & -2.0001 \end{bmatrix}, \\ \hat{\mathbf{B}}(t) &= \begin{bmatrix} 0 \\ 12.5671 + 6.2836\mathbf{c}(t) \end{bmatrix}, \\ \hat{\mathbf{C}}(t) &= [ 1 + 0.3\mathbf{c}(t) \quad 0 ]. \end{aligned} \quad (54)$$

Note that we neglected the sine terms with magnitude less than  $10^{-8}$  for the clarity. Since it is challenging to derive the Floquet transform for  $\hat{\mathbf{A}}(t)$  given in (53), we numerically computed a similarity transformation matrix that will give us the Floquet multipliers ( $\{e^{\lambda_i T}\}_{i=1}^{n_p}$ , where  $\{\lambda_i\}_{i=1}^{n_p}$  are the eigenvalues of  $\mathbf{A}$  [21]) as  $\mu_{1,2} = 0.5903 \pm 0.1419j$ . On the other hand, Floquet multipliers of  $\hat{\mathbf{A}}$ , which is computed through our subspace identification method, are  $\hat{\mu}_{1,2} = 0.5911 \pm 0.1360j$ , which are very close to numerical solution. In order to evaluate the prediction performance, we compute the normalized root mean squared error (nrms) on identification data (see Table I). We also contaminate the output data  $y(t)$  with zero mean white Gaussian noise to quantify prediction performance with different signal-to-noise (SNR) conditions. As seen in Table I, the proposed method generates accurate output predictions for noise free case. For the noisy cases, we performed 100 independent noise realizations and report mean nrms errors.

TABLE I  
NRMSE OF IDENTIFICATION DATA WITH DIFFERENT NOISE REALIZATIONS

SNR	$\infty$	40	30	20
Our Method	$10^{-8}$	0.1921	0.6417	2.4961
Verhaegen [15]	$10^{-13}$	0.9355	1.7326	3.3741

To provide a comparative analysis, we implemented the time-domain subspace identification method proposed in [15] for the same example defined in (52). We simulated (52) with a white noise sequence and collected sampled input–output data. Note that [15] works with discrete-time LTP systems. However, since we are working with sampled data, it is fair to compare input–output data of the two methods. Note that the nrms results presented in Table I for [15] are based on prediction performance of its own identification signal (noise sequence). Our method works slightly better than [15] for predicting the identification signals under different noise realizations. In addition, we tested both methods with different test signals such as a sinusoidal, noise sequence, step and square

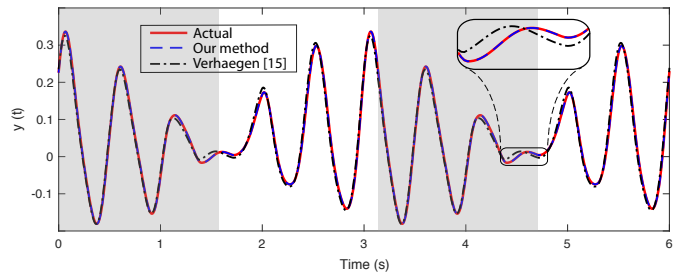


Fig. 1. Comparison of the proposed method and [15] for predicting the output of a square wave input signal with period  $\pi$ . Shaded and white regions represent the  $+0.5$  and  $-0.5$  regions of the square wave, respectively.

wave input signals (Table II). Again, the proposed method works slightly better for prediction of different test signals as compared to [15]. To illustrate, we show a comparison plot for the square wave test signal prediction performance of the two methods in Fig. 1. The minor difference in prediction performance can be spotted in this comparison plot.

TABLE II  
NRMSE FOR TEST SIGNALS

	Sinusoid	Noise	Step	Squarewave
Our Method	0.00002	0.00001	0.00003	0.00002
Verhaegen [15]	0.02020	0.00760	0.02790	0.02010

The comparison of our method with [15] reveals that both methods are accurate in predicting identification and test signals. However, we emphasize certain points for a complete discussion. First, the LTP state-space model generated by our method is more intuitive than the model obtained using [15], which seeks to find a time-invariant state-space quadruple for each discrete-time step. Therefore, for an  $N$ -periodic discrete-time LTP system, [15] generates  $N$  different state-space quadruples, which is much more difficult to interpret than the form in (54) generated by our method. Moreover, the Floquet form in (54) is more preferable due to the time-invariant state matrix. Nevertheless, even though both methods work with a single input–output data pair, [15] finds and works with the smallest data length. Therefore, [15] is more advantageous in terms of using less data.

## VI. CONCLUSION

In this note, we proposed a new method for subspace-based state-space identification of LTP systems using frequency response data. Our solution is based on the fact that LTP systems can be transformed into equivalent discrete-time LTI systems. To accomplish this, we utilize bilinear (Tustin) transformation and a frequency domain lifting method available in the literature. Then, we estimate an LTI system representation that can predict the input–output data of the original system.

We then introduced a novel method to obtain a time-periodic realization for the estimated equivalent lifted LTI system. Note that the proposed LTP realization method works with the complexity of a standard subspace identification procedure. Finally, the estimated LTP system has a time-invariant state matrix. Therefore, our method allows finding Floquet transforms for known LTP systems via system identification.

## APPENDIX A

This appendix gives a summary of implementation details.

- Simulate (1) with a sum-of-cosines input, selecting the frequencies as defined in [25].
- Obtain sampled data  $\mathbf{u}_d[k]$  and  $\mathbf{y}_d[k]$  for (3).
- Use (13) and (7) to obtain  $\mathcal{U}_d$  and  $\mathcal{Y}_d$ .
- Process each frequency separately; choose  $\bar{\mathcal{U}}_d = K$  and use (25) to obtain  $\mathcal{Y}$ .
- Combine  $\bar{\mathcal{U}}_d$  and  $\mathcal{Y}$  for each frequency in vectors and use CVA [18] to obtain (30) (backsubstitute  $\mathcal{T}_x$  and  $\mathcal{T}_y$ ).
- Perform eigenvalue decomposition on  $\hat{A}$  and perform the similarity transformation in (32).
- Construct the constraint equation in (42) and use SVD to find the nullspace vectors.
- Choose a solution from the nullspace and do the similarity transformation in (48) to obtain (49).
- Use (50) as the inverse bilinear (Tustin) transform.

## ACKNOWLEDGMENT

Authors thank Orhan Arıkan, Hasan Hamzaçebi and Ahmet D. Sezer for their invaluable ideas. We also thank the Editor and the reviewers for their constructive comments which greatly improved the quality of the manuscript. This material is based upon work supported in part by the National Science Foundation under Grant No. 1557858 to Noah J. Cowan.

## REFERENCES

- [1] L. Mevel, I. Gueguen, and D. Tcherniak, "LPTV subspace analysis of wind turbines data," in *Proc of the European Workshop on Structural Health Monitoring*, 2014.
- [2] M. S. Allen, "Frequency-domain identification of linear time-periodic systems using LTI techniques," *J Comput Nonlin Dyn*, vol. 4, no. 4, p. 041004, 2009.
- [3] A. Fujimori and L. Ljung, "A polytopic modeling of aircraft by using system identification," in *Proc Int Conf of Control and Automation*, vol. 1, Budapest, Hungary, 2005, pp. 107–112.
- [4] D. Logan, T. Kiemel, and J. J. Jeka, "Using a system identification approach to investigate subtask control during human locomotion," *Front Comput Neurosci*, vol. 10, p. 146, 2017.
- [5] S. A. Burden, S. Revzen, and S. S. Sastry, "Model reduction near periodic orbits of hybrid dynamical systems," *IEEE T Automat Contr*, vol. 60, no. 10, pp. 2626–2639, 2015.
- [6] E. Mollerstedt and B. Bernhardsson, "Out of control because of harmonics—an analysis of the harmonic response of an inverter locomotive," *IEEE Contr Syst Mag*, vol. 20, no. 4, pp. 70–81, 2000.
- [7] N. M. Wereley, "Analysis and control of linear periodically time varying systems," Ph.D. dissertation, Massachusetts Institute of Technology, 1990.
- [8] H. Sandberg, E. Mollerstedt, and B. Bernhardsson, "Frequency-domain analysis of linear time-periodic systems," *IEEE T Automat Contr*, vol. 50, no. 12, pp. 1971–1983, 2005.
- [9] S. Bittanti, G. Fronza, and G. Guardabassi, "Periodic control: a frequency domain approach," *IEEE T Automat Contr*, vol. 18, no. 1, pp. 33–38, 1973.
- [10] S. Bittanti and P. Colaneri, "Invariant representations of discrete-time periodic systems," *Automatica*, vol. 36, no. 12, pp. 1777–1793, 2000.
- [11] S. J. Shin, C. E. Cesnik, and S. R. Hall, "System identification technique for active helicopter rotors," *J Intel Mat Syst Str*, vol. 16, no. 11-12, pp. 1025–1038, 2005.
- [12] I. Uyanik *et al.*, "Identification of a vertical hopping robot model via harmonic transfer functions," *T I Meas Control*, vol. 38, no. 5, pp. 501–511, 2016.
- [13] —, "Toward data-driven models of legged locomotion using harmonic transfer functions," in *Proc IEEE Int Conf on Advanced Robotics*, 2015, pp. 357–362.
- [14] M. M. Ankarali and N. J. Cowan, "System identification of rhythmic hybrid dynamical systems via discrete time harmonic transfer functions," in *Proc IEEE Int Conf on Decision and Control*, LA, CA, USA, 2014.
- [15] M. Verhaegen and X. Yu, "A class of subspace model identification algorithms to identify periodically and arbitrarily time-varying systems," *Automatica*, vol. 31, no. 2, pp. 201–216, 1995.
- [16] Z. Shi, S. Law, and H. Li, "Subspace-based identification of linear time-varying system," *AIAA J*, vol. 45, no. 8, pp. 2042–2050, 2007.
- [17] P. Van Overschee and B. De Moor, *Subspace identification for linear systems: Theory–Implementation–Applications*. Springer Science & Business Media, 2012.
- [18] W. E. Larimore, "Canonical variate analysis in identification, filtering, and adaptive control," in *Proc IEEE Int Conf on Decision and Control*, 1990, pp. 596–604.
- [19] J. Goos and R. Pintelon, "Continuous-time identification of periodically parameter-varying state space models," *Automatica*, vol. 71, pp. 254–263, 2016.
- [20] I. Uyanik *et al.*, "Parametric identification of hybrid linear-time-periodic systems," *IFAC-PapersOnLine*, vol. 49, no. 9, pp. 7–12, 2016.
- [21] M. Farkas, *Periodic motions*. Springer Science & Business Media, 2013, vol. 104.
- [22] P. Van Overschee and B. De Moor, "Continuous-time frequency domain subspace system identification," *Signal Process*, vol. 52, no. 2, pp. 179–194, 1996.
- [23] R. Tóth, P. Heuberger, and P. Van den Hof, "Discretisation of linear parameter-varying state-space representations," *IET Control Theory A*, vol. 4, no. 10, pp. 2082–2096, 2010.
- [24] I. Uyanik, "Identification of legged locomotion via model-based and data-driven approaches," Ph.D. dissertation, Bilkent University, 2017.
- [25] M. K. Vakilzadeh *et al.*, "Experiment design for improved frequency domain subspace system identification of continuous-time systems," *IFAC-PapersOnLine*, vol. 48, no. 28, pp. 886–891, 2015.
- [26] E. K. Hidir, I. Uyanik, and Ö. Morgül, "Harmonic transfer functions based controllers for linear time-periodic systems," *T I Meas Control*, 2018.
- [27] T. McKelvey, H. Akçay, and L. Ljung, "Subspace-based multivariable system identification from frequency response data," *IEEE T Automat Contr*, vol. 41, no. 7, pp. 960–979, 1996.
- [28] H. Akçay, "Frequency domain subspace-based identification of discrete-time singular power spectra," *Signal Process*, vol. 92, no. 9, pp. 2075–2081, 2012.
- [29] A. Jhinaoui, L. Mevel, and J. Morlier, "Subspace identification for linear periodically time-varying systems," *IFAC Proceedings Volumes*, vol. 45, no. 16, pp. 1282–1287, 2012.
- [30] T. McKelvey and H. Akçay, "An efficient frequency domain state-space identification algorithm," in *Proc IEEE Int Conf on Decision and Control*, vol. 4, Lake Buena Vista, FL, USA, 1994, pp. 3359–3364.
- [31] J.-W. van Wingerden, F. Felici, and M. Verhaegen, "Subspace identification of MIMO LPV systems using a piecewise constant scheduling sequence with hard/soft switching," in *Proc IEEE European Control Conf*, Kos, Greece, 2007, pp. 927–934.
- [32] M. Verhaegen and P. Dewilde, "Subspace model identification part 1. the output-error state-space model identification class of algorithms," *Int J Control*, vol. 56, no. 5, pp. 1187–1210, 1992.
- [33] R. Pintelon, "Frequency-domain subspace system identification using non-parametric noise models," *Automatica*, vol. 38, no. 8, pp. 1295–1311, 2002.
- [34] W. Favoreel *et al.*, "Comparative study between three subspace identification algorithms," in *Proc of IEEE European Control Conf*, 1999, pp. 821–826.
- [35] A. Varga, "Computational issues for linear periodic systems: paradigms, algorithms, open problems," *Int J Control*, vol. 86, no. 7, pp. 1227–1239, 2013.
- [36] I. Markovskiy, J. Goos, K. Usevich, and R. Pintelon, "Realization and identification of autonomous linear periodically time-varying systems," *Automatica*, vol. 50, no. 6, pp. 1632–1640, 2014.